

The Anionic Superconductor $\text{Bi}_3\text{BaO}_{5.5}$: A bcc Structure Closely Related to the Perovskite. Relationships with Anti α -AgI

C. Michel,¹ D. Pelloquin, M. Hervieu, and B. Raveau

Laboratoire CRISMAT associé au CNRS, ISMRa/Université de Caen, Boulevard du Maréchal Juin 14050 Caen Cedex, France

and

F. Abbattista and M. Vallino

Dipartimento di Scienza dei Materiali e Ingegneria Chimica, Politecnico di Torino, Turin, Italy

Received April 16, 1993; in revised form July 1, 1993; accepted July 7, 1993

The average bcc structure of $\text{Bi}_3\text{BaO}_{5.5}$ ($a = 4.3822(2) \text{ \AA}$) has been determined by powder neutron diffraction. The calculations performed in the space group $Im\bar{3}m$ have shown that the Bi and Ba atoms are statistically distributed over the $2(a)$ sites (0, 0, 0), whereas oxygen and anionic vacancies are statistically distributed over the $6(b)$ sites ($\frac{1}{2}, 0, 0$). The cationic positions and the large anisotropic thermal factors of the oxygen atoms resemble the anti α -AgI structure. However, the anionic positions correspond to those observed in the perovskite. Thus, contrary to $\text{Cd}_{0.79}\text{Cd}_{0.21}\text{O}_{1.39}$, this phase cannot be considered as an anti α -AgI structure. It can better be described as the coexistence of the two configurations of the perovskite inside the crystals. Ionic conductivity measurements show that this phase is an anionic conductor with an activation energy of 0.90 eV and $T_{673 \text{ K}} \approx 10^{-3} \Omega^{-1} \text{ cm}^{-1}$. © 1994 Academic Press, Inc.

INTRODUCTION

Bismuth-based oxides are interesting materials owing to their ability to exhibit either superconducting properties or anionic conductivity. Although it has been extensively studied, the ternary system Ba-Bi-O is far from being understood. The perovskite BaBiO_3 has indeed been the subject of many papers, with much of controversy (1-9). It is now well established that this oxide with a monoclinic symmetry exhibits two different structural arrangements due to order-disorder phenomena (8, 9). Nevertheless, Saponov *et al.* (10) have recently claimed for the perovskite structure a very large homogeneity range from $\text{Ba}_{0.21}\text{Bi}_{0.79}\text{O}_x$ to $\text{Ba}_{0.63}\text{Bi}_{0.37}\text{O}_y$. In fact the study of the bismuth-rich compositions and especially of $\text{Bi}_3\text{BaO}_{5.5}$ by X-ray and electron diffraction (11) shows that the struc-

ture of these phases is more complex than expected. $\text{Bi}_3\text{BaO}_{5.5}$ exhibits indeed at least three crystallographic forms whose X-ray diffraction patterns are related to those of the perovskite. The simplest form is cubic with a parameter close to the perovskite ($a \approx 4.38 \text{ \AA}$); nevertheless it differs from the perovskite by the conditions of reflection ($h + k + l + 2n$), which implies a bcc cell instead of a primitive cell classically observed for the perovskite. Moreover, weak incommensurate satellites are observed on the electron diffraction (ED) patterns of this phase. A similar bcc cell was previously observed for the oxide $\text{Bi}_{0.79}\text{Cd}_{0.21}\text{O}_{1.395}$ (12). The X-ray diffraction study of a single crystal of the latter phase has shown that it exhibits an anti α -AgI structure, with metallic atoms statistically distributed over the two cationic positions of the cubic ABO_3 perovskite, but with oxygen atoms sitting significantly far from the classical anionic positions of the cubic perovskite. In order to understand the relationships between $\text{Bi}_3\text{BaO}_{5.5}$, the anti α -AgI, and perovskite structures, it is absolutely necessary to determine the oxygen positions with accuracy. In the present paper we describe the structure of the cubic form of $\text{Bi}_3\text{BaO}_{5.5}$ determined from powder neutron diffraction data and the anionic conduction properties of this oxide.

EXPERIMENTAL

As described previously (11), the cubic form of $\text{Bi}_3\text{BaO}_{5.5}$ was prepared from a mixture of Bi_2O_3 and $\text{Ba}(\text{NO}_3)_2$, both analytical grade quality, with the ratio Bi/Ba = 3. The reactants were mixed by grinding them with acetone in an agate mortar and pestle. After evaporation of the organic solvent, the mixture was pressed into pellets and calcined in air at about 650°C for several hours. Then it was reground, repelletized, heated at 730°C in a silver

¹ To whom correspondence should be addressed.

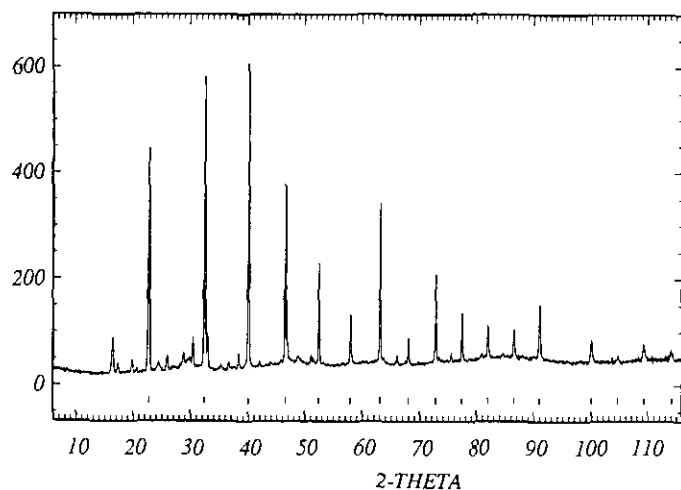


FIG. 1. Powder neutron diffraction pattern of Bi₃BaO_{5.5} ($\lambda = 1.2268$ Å). The marks correspond to Bragg angles for the body centered cubic cell.

vessel for 48 h, and then quenched down to room temperature.

Powder neutron diffraction data were collected on the 3T2 diffractometer ($\lambda = 1.2268$ Å) at the Laboratory Leon Brillouin (Saclay) over an angular range of $6^\circ \leq 2\theta \leq 116^\circ$ at increments of 0.05° (2θ). The profile refinement computer program DBW 3.2 (13) was used for the calculations. Scattering lengths were 0.5250, 0.8526, and 0.5805 (in 10^{-12} cm) for Ba, Bi, and O, respectively (14). The ionic conductivity was measured using the complex independence method by means of a Schlumberger 4415 frequency generator and a Tekelec autophase TE 9700 lock-in amplifier. Measurements were performed in air on sintered pellets (12 mm diameter, 2 mm thickness) from room temperature to about 400°C using blocking electrode in silver paste.

RESULTS AND DISCUSSION

The powder neutron diffraction (ND) pattern of the cubic form of Bi₃BaO_{5.5} (Fig. 1) shows only weak lines other than those of the body-centered cubic cell with $a = 4.3822(2)$ Å. The latter can easily be assigned to satellites in incommensurate positions as previously shown by electron diffraction (11). In every microcrystal, a modulation occurs along the three $\langle 100 \rangle_p^*$, leading to a periodicity close to 2.6. Thus on the basis of the ED patterns, the weak extra lines of the ND pattern can be indexed with six indices h, k, l, m, n, p , using the relation $1/d^2 = (1/a^2) [(h \pm m/q)^2 + (k \pm n/q)^2 + (l \pm p/q)^2]$, and with the conditions of reflection $h + k + l + m + n + p = 2n$. The best fit is obtained for $1/q = 0.364$ (Table 1).

The weak intensities of the incommensurate extra reflections from ND data, as well as from ED patterns,

TABLE 1
BaBi₃O_{5.5}: Proposed Indexation of the Neutron Diffraction Pattern ($\lambda = 1.2268$ Å)

$2\theta_{\text{exp}}$	$2\theta_{\text{cal}}$	I/I_0^a	h	k	l	m	n	p
16.54	16.52	12	1	1	0	$\bar{2}$	0	0
17.45	17.49	4	0	0	0	2	2	0
19.88	19.86	5	2	0	0	$\bar{2}$	0	0
20.65	20.68	1	0	1	1	$\bar{2}$	$\bar{2}$	0
*22.83 ^b	22.83	73	1	1	0	0	0	0
24.45	24.48	3	1	1	0	$\bar{1}$	1	0
26.02	26.03	4	0	1	1	2	0	0
28.89	28.91	4	1	1	0	$\bar{2}$	2	0
29.86	29.87	2	1	0	0	1	3	1
30.47	30.44	9	2	1	1	$\bar{2}$	0	0
*32.51	32.51	96	2	0	0	0	0	0
33.00	33.03	11	1	1	0	2	0	0
35.33	35.32	1	1	2	1	2	$\bar{2}$	$\bar{2}$
36.67	36.68	1	1	2	1	$\bar{2}$	0	0
38.41	38.39	5	2	2	0	$\bar{2}$	0	0
*40.09	40.10	100	2	1	1	0	0	0
42.05	42.06	1	3	0	1	$\bar{2}$	2	0
43.98	43.92	<1	1	2	2	1	$\bar{1}$	$\bar{1}$
45.85	45.85	<1	2	1	0	1	1	1
*46.64	46.64	58	2	2	0	0	0	0
47.00	47.03	7	1	2	1	2	0	0
48.83	48.82	2	1	2	1	$\bar{2}$	2	0
51.16	51.17	3	2	2	2	$\bar{2}$	0	0
51.52	51.53	2	1	0	3	$\bar{2}$	$\bar{2}$	0
*52.53	52.54	33	3	1	0	0	0	0
*58.01	58.01	16	2	2	2	0	0	0
58.28	58.34	1	1	3	0	2	0	0
62.25	62.27	3	2	1	3	$\bar{2}$	2	0
*63.16	63.17	51	3	2	1	0	0	0
63.71	63.69	1	3	2	0	1	$\bar{1}$	1
66.12	66.14	3	3	0	1	2	0	0
67.53	67.54	<1	3	2	1	$\bar{2}$	2	2
*68.09	68.10	9	4	0	0	0	0	0
*72.86	72.86	28	3	3	0	0	0	0
			4	1	1	0	0	0
73.42	73.42	1	2	2	1	4	1	$\bar{2}$
75.59	75.59	3	3	2	0	2	$\bar{1}$	$\bar{4}$
*77.50	77.51	16	4	2	0	0	0	0
80.98	80.98	1	2	4	2	$\bar{2}$	0	0
*82.05	82.07	10	3	3	2	0	0	0
84.63	84.59	<1	4	1	0	2	$\bar{1}$	0
*86.58	86.59	9	4	2	2	0	0	0
*91.06	91.08	17	4	3	1	0	0	0
			5	1	0	0	0	0
*100.10	100.11	7	5	2	1	0	0	0
*104.68	104.71	1	4	4	0	0	0	0
*109.38	109.41	5	4	3	3	0	0	0
			5	3	0	0	0	0
*114.20	114.25	2	4	4	2	0	0	0
			6	0	0	0	0	0

Note. For signification of indices, see text.

^a Peak height.

^b Asterisk denotes reflections corresponding to the cubic cell without modulation.

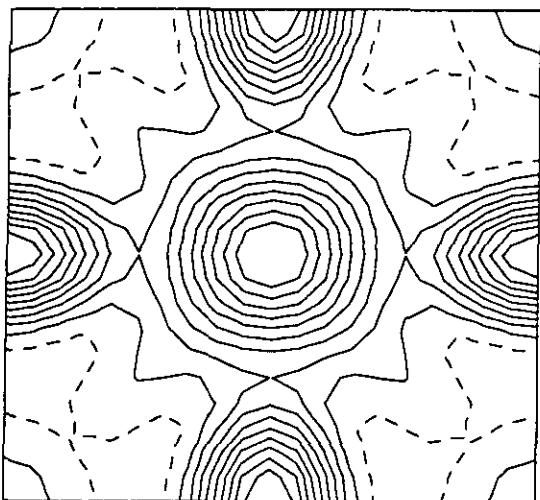


FIG. 2. Fourier difference map in the (xoy) plane, at level $z = 0$, showing peaks at $\frac{1}{2}, 0, 0$; $0, \frac{1}{2}, 0$; and $\frac{1}{2}, \frac{1}{2}, 0$, and strong anisotropy.

suggest that it should be possible to determine the average structure of this oxide in the bcc cubic cell ($a = 4.382 \text{ \AA}$), with the space group $Im\bar{3}m$. Background parameters were manually determined and a pseudo-Voigt function was used for peak profile calculations. Barium and bismuth atoms were first distributed over the $2(a)$ sites of this group $(0, 0, 0; \frac{1}{2}, \frac{1}{2}, \frac{1}{2})$ which correspond to the cationic positions in both structures, anti α -AgI and perovskite. Fourier difference series performed at this stage of the investigation show peaks centered on the $6(b)$ positions $(\frac{1}{2}, \frac{1}{2}, 0; \frac{1}{2}, 0, 0)$ and were characterized by a strong anisotropy (Fig. 2). The latter were attributed to oxygen atoms. Thus the $6(b)$ sites were supposed to be less than half occupied statistically by oxygen atoms according to the cell content: $Ba_{0.5}Bi_{1.5}O_{2.75}$. Under these conditions, the isotropic thermal factors were refined, leading to a R_1 factor of 15% for an abnormally high B factor of oxygen, $B = 14 \text{ \AA}^2$ (Table 2, column 1). At this stage, refining the occupancy factor of the anionic site did not change the

TABLE 2
 $BaBi_3O_{5.5}$: Refined Parameters and Agreement Factors Obtained for Several Hypotheses (See Text)

		(1)	(2)	(3)
Ba/Bi	$B(\text{\AA})^2$	2.51 (6)	2.58 (4)	2.59 (4)
O	$B(\text{\AA})^2$	14.0 (3)	^a	^b
	N	2.75	2.78 (6)	2.77 (4)
R_p (%)		8.43	5.90	4.68
R_{wp} (%)		13.00	9.10	5.81
R_i (%)		15.04	5.24	3.39

^a $\beta_{11} = \beta_{22} = 0.281$ (7), $\beta_{33} = 0.067$ (5).

^b $\beta_{11} = \beta_{22} = 0.285$ (5), $\beta_{33} = 0.067$ (3).

TABLE 3
Observed and Calculated Integrated Intensities for $BaBi_3O_{5.5}$ as Calculated by the Program

h	k	l	I_{obs}	I_{calc}	h	k	l	I_{obs}	I_{calc}
1	1	0	138	140	3	3	2	18	22
2	0	0	158	160	4	2	2	16	15
2	1	1	158	155	4	3	1	10	9
2	2	0	85	87	5	1	0	26	24
3	1	0	47	48	5	2	1	17	16
2	2	2	24	26	4	4	0	4	4
3	2	1	76	77	4	3	3	7	9
4	0	0	13	14	5	3	0	7	9
3	3	0	12	12	4	4	2	2	2
4	1	1	34	33	6	0	0	6	7
4	2	0	26	26					

oxygen content significantly, confirming the results of the chemical analysis. Taking into consideration the results of the Fourier difference series, the anisotropic thermal factors of oxygen were then refined, leading to a dramatic decrease of the R_1 factor to 5%, without changing the oxygen content significantly (Table 2 column 2). In order to test the influence of the modulation lines, on the R factors, some of these lines which slightly overlap with the main peaks (for $2\theta = 33.00, 47.00, 58.28, 63.71$, and 73.42°) were manually deleted in a last refinement. The R factors were then lowered without any significant variation of the various parameters (Table 2 column 3). The observed and calculated intensities are given in Table 3.

Attempts to locate the oxygen atoms on the $12(d)$ positions $(\frac{1}{4}, 0, \frac{1}{2})$, as in $Bi_{0.79}Cd_{0.27}O_{1.395}$ (12), led to a dramatic increase of the R factors in agreement with the Fourier difference results. Similarly, attempts to split the $6(b)$ positions into $24(h)$ $(0, x, x)$ or into $24(g)$ $(x, 0, \frac{1}{2})$ positions as Ag in the α -AgI structure, determined by neutron diffraction at several temperatures (15), always led to an increase of the R factors without changing significantly the atomic parameters.

This structural study confirms our previous model related to the perovskite structure. $BaBi_3O_{5.5}$ (Fig. 3a), contrary to $Bi_{0.79}Cd_{0.27}O_{1.395}$ (12) (Fig. 3b), cannot be considered an anti α -AgI structure. The Bi and Ba atoms are, like the Bi and Cd atoms, located on the iodine sites of the α -AgI structure, but the oxygen atoms do not sit on the $24(g)$ sites. On the contrary, they are distributed over the $6(b)$ sites which correspond to the two classical representations of the perovskite structure (Figs. 4a and b), suggesting that these two kinds of configurations coexist in the same crystal (Fig. 4c). Nevertheless, an interesting analogy with the α -AgI structure deals with the abnormally high anisotropic factors of oxygen, which are similar to those of silver. For the $\frac{1}{2}, \frac{1}{2}, 0$ positions the amplitude of the vibration is about 0.53 \AA along \bar{a} and \bar{b} , and 0.25

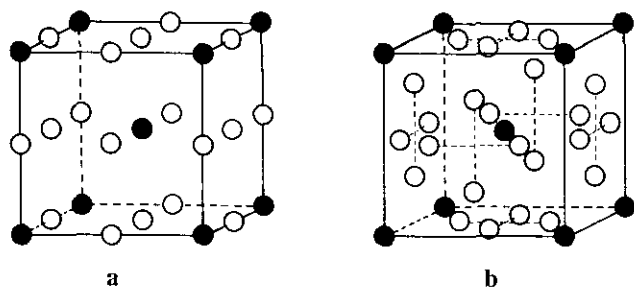


FIG. 3. Structure of $\text{BaBi}_3\text{O}_{5.5}$ (a) and of $\text{Bi}_{0.79}\text{Cd}_{0.27}\text{O}_{1.397}$ (b). Filled and open circles represent metals (mixed Ba, Bi and Bi, Cd) and oxygen positions, respectively.

Å along \tilde{c} . This suggests a large possibility of delocalization of oxygen over the anionic sites leading, as for $\alpha\text{-AgI}$, to ionic conductivity. It is likely that adjacent 6(b) sites cannot be occupied simultaneously owing to the too short O–O distances (2.19 Å). In the same way the coexistence of a barium atom in (0, 0, 0) and of an oxygen atom in $(\frac{1}{2}, 0, 0)$ would lead to an abnormally short Ba–O distance (2.19 Å). This implies a modulated distribution of the cations and of the anions over their respective sublattices in agreement with the existence of incommensurate satellites. Such a modulation supports our model of the coexistence of the two configurations of the cubic perovskite in the same crystal (Fig. 4c). In this way, the M –O distances of 2.19 and 3.09 Å correspond to $M = \text{Bi(III)}$ and Ba, respectively. The rather high isotropic thermal factors of bismuth and barium, $B = 2.5\text{--}2.6 \text{ \AA}^2$, can be compared with those obtained in the system $\text{Bi}_2\text{O}_3\text{--Y}_2\text{O}_3$, i.e., 1.71–2.1 Å^2 (16) and in the oxide $\text{Bi}_{0.7}\text{La}_{0.3}\text{O}_{1.5}$, i.e., 1.59–2.53 Å^2 (17).

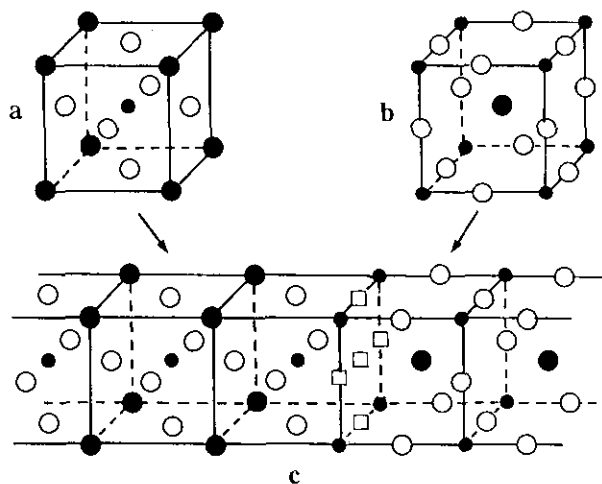


FIG. 4. (a, b) The two classical representations of the perovskite structure; (c) possible arrangement at the junction of two domains. Large and small filled circles, open circles, and open squares represent Ba, Bi, O, and vacancies respectively.

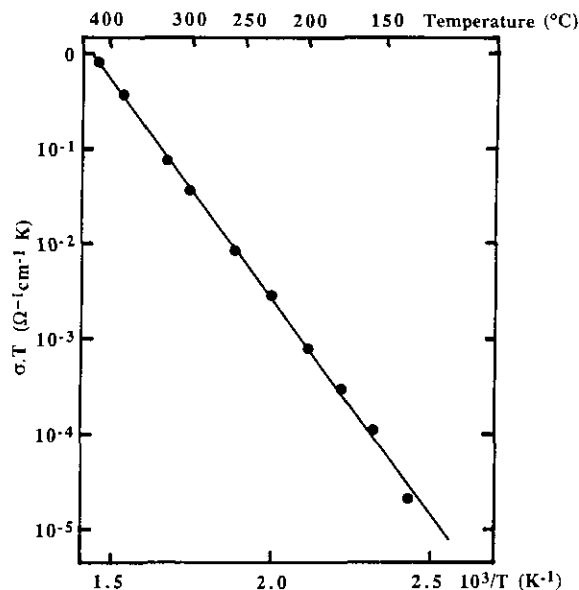


FIG. 5. Logarithmic plot of $\sigma T = f(1/T)$ obtained from complex independence measurements.

An interesting feature of this structure deals with the existence of anionic vacancies: one site out of 12 is vacant with respect to the stoichiometric perovskite ABO_3 . This led us to the investigation of the ionic conduction properties of this phase. The measurements were performed in air versus temperature. At room temperature the resistance of the sample is too high to be measured. The highest temperature was limited at about 400°C in order to avoid a possible transformation of the structure. After measurements, the pellet was ground and the XRD pattern did not reveal any phase transformation. The logarithmic plot $\sigma T = f(1/T)$ (Fig. 5) exhibits a linear variation with an activation energy of 0.90 eV and $\sigma_{673\text{K}} \sim 10^{-3} \Omega^{-1}\text{cm}^{-1}$. These values are very similar to those observed for $(\text{Bi}_2\text{O}_3)_{0.8}(\text{BaO})_{0.2}$ (18) ($\sigma_{673\text{K}} = 2.10^{-3} \Omega^{-1}\text{cm}^{-1}$, $\Delta E \approx 1 \text{ eV}$); the conductivity of this phase, calculated by extrapolation, is higher than that of stabilized zirconia ($\sigma_{1273\text{K}} = 5.10^{-2} \Omega^{-1}\text{cm}^{-1}$) which exhibits a similar activation energy of 1 eV. On the contrary, the oxide $\text{Bi}_{1-x}\text{Cd}_x\text{O}_{1.5-x/2}$ exhibits a much higher conductivity ($10^{-1} \Omega^{-1}\text{cm}^{-1} < \sigma_{673} < 1 \Omega^{-1}\text{cm}^{-1}$), depending on composition, and lower activation energy ($E_a \sim 0.3 \text{ eV}$) (19); nevertheless, predominance of electronic conductivity was evident in the bismuth cadmium oxides (20), making the comparison difficult. The examination of the structure suggests a hopping conductivity. Using this model, if one applies the expression $\sigma = (Nq^2a^2\nu/3kT) \exp(-E_a/kT)$ (21), where N is the density of mobile ions (O^{2-}), q their charge, a the jump distance, and ν the jump frequency which can be deduced from the frequency at the resonance ($\nu \sim 1.8 \cdot 10^{13} \text{ sec}^{-1}$), we obtain $a \sim 4.6 \text{ \AA}$. This value, close to that

of the lattice parameter (4.38 Å), has to be compared with the jump distance in α -AgI (~ 5 Å), which is also close to that of the cell constant (5.06 Å).

CONCLUDING REMARKS

This study shows that the bcc form of $\text{Bi}_3\text{BaO}_{5.5}$ is an ionic conductor. The study demonstrates that, despite its apparent similarity with the anti α -AgI structure, it does not really belong to this family, and that it should better be considered as derived from the perovskite. In this respect it exhibits a different behavior from $\text{Bi}_{0.79}\text{Cd}_{0.21}\text{O}_{1.395}$ (12), which is characterized by an anti α -AgI structure. It is worth pointing out that several other oxides characterized by a similar bcc structure have been isolated previously in the systems Bi_2O_3 -AO with $A = \text{Ca}(22)$, $\text{Sr}(23)$, $\text{Pb}(24)$, and Ba , Na , K , and $\text{Mn}(25)$. In the case of barium, a difference with regard to silver iodide structure was suggested by Raman spectroscopy (25). A systematic neutron diffraction study of these phases is necessary to understand their relationships with the perovskite and anti α -AgI structures.

ACKNOWLEDGMENT

The authors are grateful to Dr. F. Bourée (Laboratoire L. Brillouin, Saclay) for neutron diffraction facilities.

REFERENCES

1. E. T. Shuvaeva and E. G. Fesenko, *Sov. Phys.—Crystallogr. (Engl. Transl.)* **14**, 926 (1970).
2. Y. N. Venevstev, *Mater. Res. Bull.* **6**, 1085 (1971).
3. T. Nakamura, S. Kose, and T. Sata, *J. Phys. Soc. Jpn.* **31**, 1284 (1971).
4. D. E. Cox and A. W. Sleight, *Solid State Commun.* **19**, 696 (1976).
5. R. Arpe and H. K. Müller-Buschbaum, *Z. Anorg. Allg. Chem.* **434**, 73 (1977).
6. G. Thornton and A. J. Jacobson, *Acta Crystallogr., Sect. B* **34**, 351 (1978).
7. D. E. Cox and A. W. Sleight, *Acta Crystallogr., Sect. B* **35**, 1 (1979).
8. C. Chaillout, J. P. Remeika, A. Santoro, and M. Marezio, *Solid State Commun.* **56**, 829 (1985).
9. C. Chaillout, A. Santoro, J. P. Remeika, A. S. Cooper, G. P. Espinosa, and M. Marezio, *Solid State Commun.* **65**, 1363 (1988).
10. V. V. Saponov, P. Kostic, I. Krstanovic, and M. M. Ristic, *Silic. Ind.* **5-6**, 165 (1990).
11. F. Abbattista, M. Hervieu, M. Vallino, C. Michel, and B. Raveau, *J. Solid State Chem.*, **104**, 338 (1993).
12. T. Graja, P. Conflant, G. Nowogrocki, J. C. Boivin, and D. Thomas, *J. Solid State Chem.* **63**, 160 (1986).
13. D. B. Wiles and R. A. Young, *J. Appl. Crystallogr.* **14**, 149 (1981).
14. Chalk River Nuclear Lab. Internal Report. AECL, 8490 (1984).
15. A. F. Wright and B. E. F. Fender, *J. Phys. C* **10**, 2261 (1977).
16. P. D. Battle, C. R. A. Catlow, J. W. Heap, and L. M. Moroney, *J. Solid State Chem.* **63**, 8 (1986).
17. D. Mercurio, M. El Farissi, J. C. Champarnaud-Mesjard, B. Frit, P. Conflant, and G. Roult, *J. Solid State Chem.* **80**, 133 (1989).
18. T. Takahashi and H. Iwahara, *Mater. Res. Bull.* **13**, 1447 (1978).
19. J. C. Boivin and P. Conflant, private communication.
20. T. Takahashi, H. Iwahara, and Y. Nagai, *J. Electrochem. Soc.* **117**, 244c (1970).
21. T. Wong, M. Brodwin, D. F. Shriver, and J. I. McOmber, *Solid State Ionics* **3-4**, 53 (1981).
22. P. Conflant, J. C. Boivin, and D. Thomas, *J. Solid State Chem.* **18**, 133 (1976).
23. R. Guillermo, P. Conflant, J. C. Boivin, and D. Thomas, *Rev. Chim. Miner.* **15**, 153 (1978).
24. F. Honnart, J. C. Boivin, D. Thomas, and K. J. de Vries, *Solid State Ionics* **9-10**, 921 (1983).
25. U. Delicat, K. Gruber, A. Püttner, E. J. Zehnder, and M. Trömel, *J. Solid State Chem.* **102**, 209 (1993).